JOURNAL OF CATALYSIS 57, 287–295 (1979)

Study of Metal Oxide Catalysts in the Olefin Oxidation from their Reduction Behavior

I. Reduction of Various Metal Oxides with Propylene

ISAO ASO, MASASHI NAKAO, NOBORU YAMAZOE, AND TETSURO SEIYAMA

Department of Materials Science and Technology, Faculty of Engineering, Kyushu University, Higashi-ku, Fukuoka, 812 Japan

Received May 19, 1978; revised November 20, 1978

The reduction behavior of 14 metal oxides with propylene was investigated to characterize their catalytic properties in the olefin oxidation. Metal oxides were classified depending on whether the reduction was limited within a few surface layers (group (I) oxides: TiO_2, Cr_2O_3, ZnO, In_2O_3, SnO_2, and WO_3) or it proceeded into the bulk (group (II) oxides: V_2O_5, MnO_2, Fe_2O_3, Co_3O_4, NiO, Bi_2O_3, CuO, and MoO_3). The distinction was shown to result from the thermodynamic stability of metal oxides. It was found that the rate and selectivity at the initial stage of reduction were well correlated with those attained in the catalytic oxidation. The fact indicates not only that lattice oxygen participates in the catalytic oxidation but also that the reduction steps of catalysts virtually determine the catalytic rates. With the progress of reduction, the activity and selectivity changed in complex manners which were widely different for group (I) and group (II) oxides. Discussion was made on such reduction behavior from various viewpoints. An interesting case was provided by ZnO in which the reduction rate as well as the rate of 1,5-hexadiene formation went through maxima. Analyses showed that, in this case, active sites (exposed metal ions) for the propylene dimerization reaction were created by the removal of surface oxygen, and that the increase of such sites coupled by the decrease of surface active oxygen gave rise to the observed rate maxima.

INTRODUCTION

A number of selective oxidation reactions of olefins over metal oxide catalysts have been recognized to proceed by a redox mechanism, for which lattice oxygen rather than adsorbed oxygen is more important. To support this mechanism, the reduction of metal oxides with olefins has been investigated successfully (*1*). Batist *et al.* (*2*) have found that the initial rate of butadiene formation in the reduction of $Bi_2O_3 \cdot MoO_3$ with 1-butene coincides with the rate of butadiene formation in the catalytic oxidation. Our study (*3*) on propylene oxidation over Bi_2O_3–MoO_3 has shown that the activation energy and the selectivity for acrolein formation in the initial stage of reduction reaction agree well with those of the catalytic reaction, respectively, indicating the participation of lattice oxygen in the catalytic oxidation. However, it has also been found that the activity and the selectivity for acrolein formation pass through maxima in the course of the reduction reaction (*3*). Such reduction behavior seems to be related not only to changes in availability of lattice oxygen but also to changes in adsorption and/or reactivity of olefins on the catalyst surface. A few reports from this standpoint were recently published on some metal oxides (*4–6*), but the subject has hardly been fully explored. In

0021-9517/79/050287-09$02.00/0

the present paper, the reduction of metal oxides with propylene was studied systematically for the further understanding of their catalytic properties. Taking ZnO as an example, it was also attempted to analyze the reduction behavior in terms of the changes of surface concentrations of available lattice oxygen and olefin adsorption sites.

EXPERIMENTAL

Preparation of Oxides

Of the 14 metal oxides used, TiO_2, In_2O_3, SnO_2, WO_3, MnO_2, and Fe_2O_3 were chemical reagents of extra-pure grade. Cr_2O_3, ZnO, Co_3O_4, Bi_2O_3, and CuO were prepared by thermal decomposition of metal hydroxides precipitated from aqueous solutions of metal nitrates with ammonia. V_2O_5 and NiO were obtained by thermal decomposition of ammonium methavanadate and nickel carbonate, respectively, the latter of which was precipitated from an aqueous solution of nickel nitrate with ammonium carbonate. MoO_3 was prepared by acidifying an aqueous solution of ammonium paramolybdate with nitric acid followed by thermal decomposition of the obtained precipitate.

All metal oxides were calcined at 600°C for 5 hr and subjected to structural identification by X-ray diffraction. Granules of 40 to 60 mesh were used. Surface area was measured by BET method.

Apparatus and Procedures

The reduction reaction was carried out in a conventional fixed catalyst bed made with an 8-mm i.d. Pyrex glass tube. Propylene (P_{PR}, 0.08 to 0.35 atm) was fed to the reactor after dilution with helium which had been dried and deoxygenated by passing through Molecular Sieve 5A at liquid nitrogen temperature. The contact time (W/F) was chosen at 0.5 to 2.0 g·s/cm³. The effluents were analyzed at intervals of 5 to 10 min by gas chromatography. The rate and amount of oxidic oxygen consumption were estimated from the formation rates of gaseous products by assuming stoichiometric reactions.

TABLE 1

Reduction of Metal Oxides with Propylene

Oxide (surface area in m²/g)	Temp.[a] (°C)	Maximum degree of reduction of oxide	Oxidation products during reduction[b]	Partial oxidation products at the initial stage of reduction (selectivity %)
TiO_2 (8.8)	525	within 1 layer	CO_2, HD, ACE, BEN	HD(20), ACE(14), BEN(11)
Cr_2O_3 (3.5)	550	5 ~ 6 layers	CO_2, BEN, HD	($CO_2 \simeq 100$)
ZnO (1.1)	500	2 ~ 3 layers	CO_2, BEN, ACE, HD	BEN(32), ACE(16)
SnO_2 (28.6)	500	within 1 layer	CO_2, BEN, HD, CHD	BEN(19), HD(4), CHD(2)
In_2O_3 (6.2)	500	within 1 layer	BEN, CHD, HD	BEN(49), CHD(26), HD(22)
WO_3 (4.2)	500	within 1 layer	CO_2, CO, ACE, HD	ACE(9), HD(2)
V_2O_5 (2.8)	400	V_2O_3	CO_2, ACE, BEN, HD	($CO_2 \simeq 100$)
MnO_2 (12.0)	453	γ-$Mn_2O_3 \rightarrow Mn_3O_4 \rightarrow MnO$	CO_2, CO, BEN	($CO_2 + CO \simeq 100$)
Fe_2O_3 (2.9)	400	Fe_3O_4	CO_2, ACE, BEN	ACE(3), BEN(1)
Co_3O_4 (5.2)	400	$CoO \rightarrow Co$	CO_2, HD, BEN	($CO_2 \simeq 100$)
NiO (23.5)	500	Ni	CO_2	($CO_2 \simeq 100$)
Bi_2O_3 (0.4)	525	Bi	HD, CHD, BEN, CO_2	HD(95), CHD(2), BEN(2)
CuO (1.8)	450	$Cu_2O \rightarrow Cu$	CO_2, ACR	ACR(5)
MoO_3 (0.3)	550	$Mo_{18}O_{52} \rightarrow Mo_4O_{11} \rightarrow MoO_2$	ACR, CO, CO_2	ACR(90)

[a] Reaction conditions: P_{PR}, 0.08 ~ 0.35 atm; W/F, 0.5 to 2.0 g·s/cm³.

[b] HD, 1,5-hexadiene; CHD, 1,3-cyclohexadiene; BEN, benzene; ACE, acetone; ACR, acrolein.

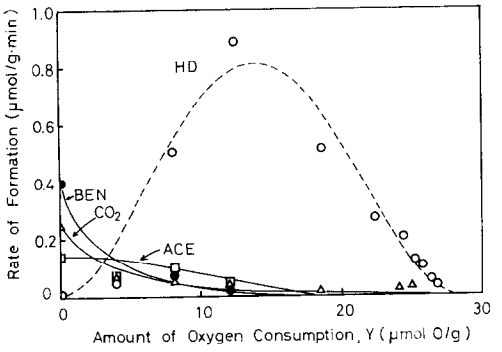

FIG. 1. Reduction of ZnO with propylene. Dotted line: see text. T, 500°C; P_{PR}, 0.15 atm; W/F, 0.5 g·s/cm³.

RESULTS

The reduction of metal oxides with propylene gave various gaseous products, i.e., 1,5-hexadiene (HD), 1,3-cyclohexadiene (CHD), benzene (BEN), acrolein (ACR), acetone (ACE), CO, and CO_2. Generally speaking, these products are essentially the same as those obtained under catalytic conditions. Table 1 summarizes the reducibility of each metal oxide (the maximum degree of reduction) and the gaseous products during as well as at the initial stage of reduction. Clearly metal oxides are classified into two groups according to whether the reduction is limited to a few surface layers (group (I)) or it extends into the bulk to give lower oxides (group (II)).

Group (I): TiO_2, Cr_2O_3, ZnO, In_2O_3, SnO_2, WO_3.

Group (II): V_2O_5, MnO_2, Fe_2O_3, Co_3O_4, NiO, Bi_2O_3, MoO_3, CuO.

It is convenient to describe experimental results according to this classification.

Reduction of Group (I) Oxides

A typical example of this group was the reduction of ZnO. The formation rates of oxidation products are depicted as a function of the amount of oxidic oxygen consumption (Y) in Fig. 1. While the formation of CO_2 decreased monotonically with an increase in Y, the partial oxidation products exhibited various behavior. Especially interesting was the behavior of 1,5-hexadiene formation, i.e., the rate went through a maximum. The total oxygen consumed (Y_∞) in this case was 28 μmol O per gram of ZnO. On assuming (10$\bar{1}$0) plane for ZnO surface, this value corresponds to the oxygen amount contained in about two surface monolayers.

The reduction of SnO_2 was limited within a surface monolayer, as shown in Fig. 2. The formation rate of benzene was largest at the onset of reduction, while those of 1,3-cyclohexadiene and 1,5-hexadiene passed through maxima. Such complex reduction behavior was also observed in the reduction of the other group (I) oxides.

As illustrated above, there was a common feature in the reduction of group (I) oxides that the formation of CO_2 decreased monotonically with the progress of reduction, while those of partial oxidation products usually attained larger or maximum rates at later reduction stages. Among partial oxidation products, moreover, there was a formation sequence, i.e., benzene, acetone, 1,3-cyclohexadiene, and 1,5-hexadiene were formed in turn in this order with the elapse of reduction time. This formation sequence coincides with the order of decreasing number of oxygen atoms being required to produce them.

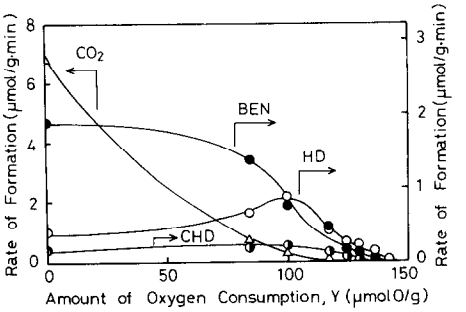

FIG. 2. Reduction of SnO_2 with propylene. T, 500°C; P_{PR}, 0.09 atm; W/F, 2.0 g·s/cm³.

Reduction of Group (II) Oxides

The rates and selectivity in the reactions between propylene and group (II) oxides were greatly different depending on metal oxide. A few examples are illustrated below.

In the reduction of Bi_2O_3, 1,5-hexadiene was produced very selectively together with small amounts of 1,3-cyclohexadiene, benzene, and CO_2. The rate of oxidic oxygen consumption decreased gradually. X-ray diffraction indicated that the reduced sample contained Bi metal and Bi_2O_3, and agromerated Bi particles were visually seen. These results agree well with those reported by Mossoth and Scarpiello (*7*) and Fattore *et al.* (*5*), except that the selectivity to the oxidative dehydrodimerization products was much higher in the present study. In contrast, the reduction of Co_3O_4 (Fig. 3), NiO, and Fe_2O_3 produced CO_2 almost exclusively. In the case of Co_3O_4, the rate first decreased rapidly to a minimum at 25% reduction (CoO composition) and there went through a maximum. NiO and Fe_2O_3 were reduced rather monotonically to Ni and Fe_3O_4, respectively.

Reduction curves became more complex for MnO_2, V_2O_5, MoO_3, and CuO. In the reduction of MnO_2 (Fig. 4), X-ray diffraction analyses indicated stepwise changes $MnO_2 \rightarrow \gamma\text{-}Mn_2O_3 \rightarrow Mn_3O_4 \rightarrow MnO$. The

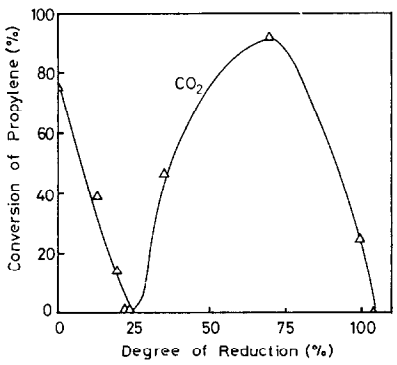

FIG. 3. Reduction of Co_3O_4 with propylene. T, 400°C; P_{PR}, 0.06 atm; W/F, 0.8 g·s/cm³.

maximum degree of reduction (ca. 42%), however, was less than 50% because the final phase, MnO, can contain large amount of nonstoichiometric oxygen: The upper limit, $MnO_{1.13}$, corresponds to 43.5% reduction of MnO_2. In contrast to the monotonous decrease of $CO_2 + CO$ formation, benzene formation showed a maximum at 33% reduction (Mn_3O_4 composition), suggesting that Mn_3O_4 is an active phase for the benzene formation. V_2O_5 was reduced to V_2O_3, though it was difficult to identify intermediate phase in between by X-ray diffraction analysis. MoO_3 was reduced to MoO_2 via $Mo_{18}O_{52}$ and Mo_4O_{11} as analyzed by X-ray diffraction, converting propylene to acrolein very selectively. Interestingly, all the gaseous products

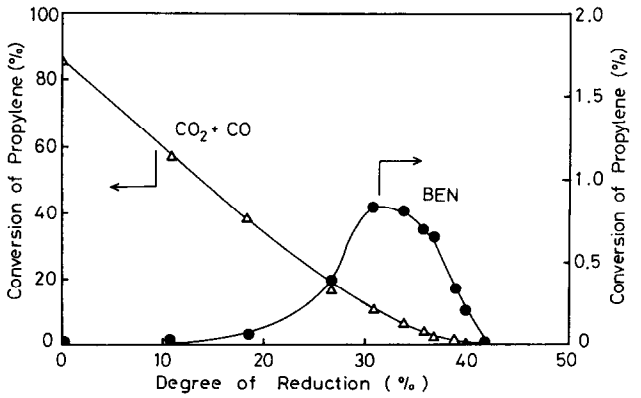

FIG. 4. Reduction of MnO_2 with propylene. T, 453°C; P_{PR}, 0.08 atm; W/F, 2.0 g·s/cm³.

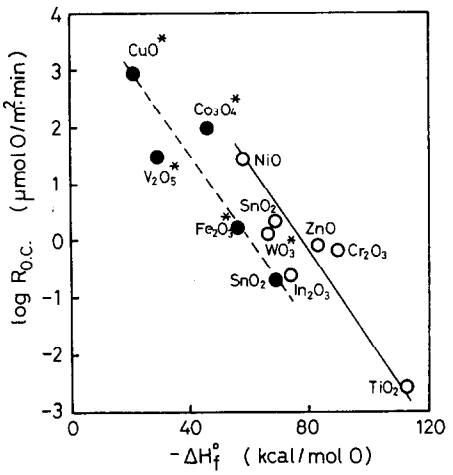

FIG. 5. Correlation between the initial rates of oxygen consumption ($R_{o.c.}$) and the heats of formation ($-\Delta H_f^\circ$) of oxides per mol O. Asterisk denotes the heat of reaction for $MO_{n-1} + \frac{1}{2}O_2 \rightarrow MO_n$. T, 500°C (——○——); 400°C(- - -●- - -).

showed two formation maxima at 2 and 20% reduction. In the case of CuO, the first reduction step $CuO \rightarrow Cu_2O$ produced CO_2 and acrolein, while the second reduction step $Cu_2O \rightarrow Cu$ produced only CO_2. The acrolein formation rate in the first step went through a maximum.

DISCUSSION

Correlation between Reduction and Catalysis

Catalytic oxidation in many cases proceeds via redox cycle, i.e., by repeating reduction and reoxidation of metal oxides with reactants and gas-phase oxygen, respectively. From this point of view, reduction behavior of oxides, as one part of the redox cycle, should reflect their catalytic properties especially at earlier stages of reduction.

The specific rates of oxygen consumption at the initial stage of reduction are plotted against the heat of oxide formation per mol O ($-\Delta H_f^\circ$) in Fig. 5. The correlations obtained indicate that the stronger the metal–oxygen bond is, the slower the rate of reduction becomes. Similar correlations have been observed in the catalytic oxidation of olefins (*8–9*). A similarity between the reduction reaction and the catalytic oxidation also exists in the selectivity to propylene oxidation products. For the catalytic propylene oxidation, we have classified oxide catalysts into acrolein-, dimer-, and CO_2-formers as shown in Table 2. The classification based on the reduction reaction is also shown in the same table. It is seen that the two classifications correspond fairly well except that many acrolein formers in the catalytic oxidation become CO_2 formers under the reductive conditions. This shift is probably caused by the difference of reaction temperature: Usually higher temperatures are necessary in the reduction reaction.

Such coincidence between the reduction reaction and the catalytic oxidation not

TABLE 2

Classification of Metal Oxide According to Selectivity of Propylene Oxidation

Reaction	Acrolein formers	Benzene or 1,5-hexadiene formers	CO_2 formers
Reduction of metal oxide[a]	MoO_3	Bi_2O_3, In_2O_3, ZnO, TiO_2, SnO_2	Co_3O_4, NiO, MnO_2, V_2O_5, Cr_2O_3, Fe_2O_3, CuO, WO_3
Catalytic oxidation over metal oxide (*9*)	MoO_3, Sb_2O_4, V_2O_5, TiO_2, Fe_2O_3, SiO_2, WO_3, Al_2O_3	ZnO, Bi_2O_3, In_2O_3, SnO_2, Ga_2O_3, CdO	highly active CuO, Co_3O_4, NiO, MnO_2, Cr_2O_3, GeO_2 slightly active CaO, MgO, CeO_2

[a] Selectivity at the initial stage of reduction.

only confirms the participation of oxidic oxygen in the catalytic oxidation, but also indicates that the cleavage of metal–oxygen bonds of catalysts is virtually rate-determining in the catalytic oxidation.

Reducibility of Metal Oxides

We have so far focused attention only at the initial stage of reduction to seek correlations with catalytic properties. In the later stage, the reduction behavior depends very much on metal oxide. We have classified metal oxides into groups (I) and (II) based on whether only the oxide surface or the bulk was reduced by propylene. This distinction is deeply connected to the thermodynamic stability of metal oxides.

Thermodynamically a reduction reaction can be divided into two steps, i.e., oxygen dissociation from a metal oxide (1) and oxygen uptake by propylene (2) as follows:

$$MO_n \rightarrow MO_{n-1} + \tfrac{1}{2}O_2 \quad \Delta G_1^\circ \quad (1)$$

$$mC_3H_6 + \tfrac{1}{2}O_2 \rightarrow \text{oxidation products} \quad \Delta G_2^\circ \quad (2)$$

$$MO_n + mC_3H_6 \rightarrow MO_{n-1} + \text{oxidation products} \quad \Delta G_3^\circ \quad (3)$$

The corresponding standard free energy changes, ΔG_1°, ΔG_2°, and ΔG_3° are related by $\Delta G_3^\circ = \Delta G_1^\circ + \Delta G_2^\circ$. ΔG_1° for various metal oxides (*10*) and ΔG_2° for typical propylene oxidation reactions (*11*) are depicted vs temperature in Fig. 6.

In the reduction of group (I) oxides, ΔG_1° is usually much larger than can be compensated by ΔG_2°, as seen in Fig. 6. This means that reaction (3) is thermo-

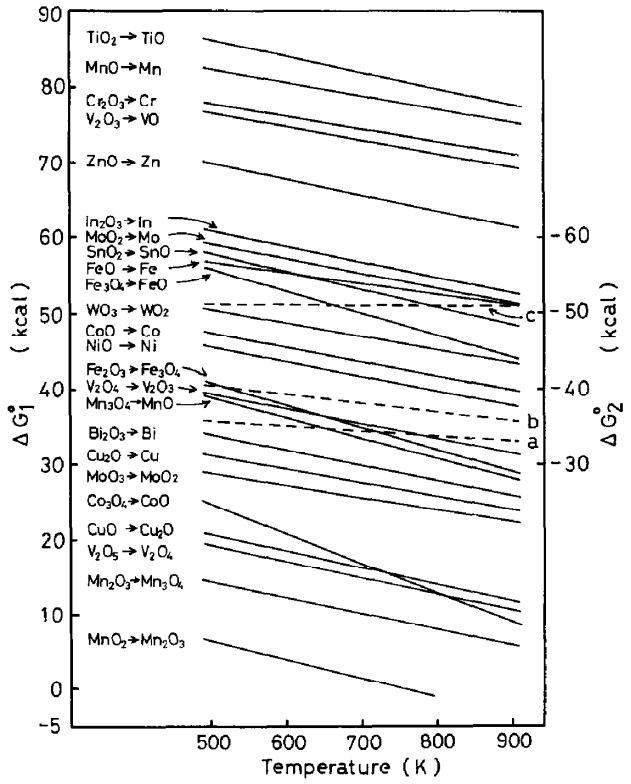

FIG. 6. Standard free energy changes of oxygen dissociation from oxide (ΔG_1°) and of propylene oxidation (ΔG_2°). ΔG_1°: step (1) for the oxide indicated in the figure. ΔG_2°: step (2) for acrolein formation (a), 1,5-hexadiene formation (b), and CO_2 formation (c).

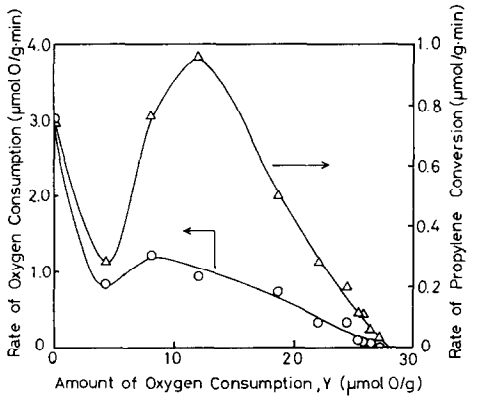

FIG. 7. Variation of the rate of oxygen consumption and the rate of propylene conversion with the amount of oxygen consumption in the reduction of ZnO. Reaction conditions: see Fig. 1.

dynamically difficult. The oxidic oxygen actually eliminated in these cases should be other than normal lattice oxygen: Weakly held surface oxygen such as adsorbed oxygen, or lattice oxygen associated with nonstoichiometry, or some sort of lattice defects should be responsible.

On the other hand, the reduction of group (II) oxides is thermodynamically favorable. Lattice oxygen is eliminated up to the bulk to form lower oxides. For instance, the free energy changes for manganese oxides at 726 K are as follows:

$$2MnO_2 \rightarrow Mn_2O_3 + \tfrac{1}{2}O_2 \quad \Delta G_1^\circ = 1 \text{ kcal}$$
$$3Mn_2O_3 \rightarrow 2Mn_3O_4 + \tfrac{1}{2}O_2 \quad = 10$$
$$Mn_3O_4 \rightarrow 3MnO + \tfrac{1}{2}O_2 \quad = 34$$
$$MnO \rightarrow Mn + \tfrac{1}{2}O_2 \quad = 79$$

ΔG_1° up to the third step can be compensated by ΔG_2° for the formation of CO_2 (-51 kcal), 1,5-hexadiene (-38 kcal), and acrolein (-35 kcal), suggesting the reduction of MnO_2 up to MnO as observed.

Reduction Behavior of Group (I) Oxides

In the reduction of group (I) oxides, propylene reacts with only limited amounts of oxygen at the oxide surface. It is expected that the concentration of such reactive surface oxygen decreases rapidly as the reduction proceeds. This explains why the deep oxidation of propylene is favored at an early stage of reduction while at later stages the partial oxidation products tend to be formed in the order of decreasing number of oxygen atoms being required.

However, the reactive oxygen concentration is not the sole important factor that determines the reduction behavior at least in the cases of ZnO and Cr_2O_3. In these cases, 1,5-hexadiene or benzene formation rates passed through very large maxima, and, in the reduction of ZnO, not only the rate of propylene conversion but also the rate of total oxygen consumption show maxima shown in Fig. 7. This fact indicates that there are certain factors which increase the reaction rate by compensating the opposite effect of the decrease in reactive oxygen concentration. The situation seems similar for the benzene formation on Cr_2O_3, though the total oxygen consumption rate showed no apparent maximum.

As stated above, the reduction behavior of ZnO appears to reflect two opposite effects. One effect, a rate-decreasing effect, apparently comes from a decrease in reactive oxygen concentration. The other, a rate-increasing effect, is proposed to arise as a result that active sites for propylene oxidation or adsorption are created. Supposedly such active sites are ascribed to the surface zinc atoms which have become exposed or coordinatively unsaturated. From these considerations, we attempted to analyze the reduction behavior of ZnO as follows.

It is assumed that propylene oxidation to a products OX takes place via surface reaction between adsorbed propylene PR_{ad} and reactive surface oxygen O_s:

$$m'PR_{ad} + n'O_s \rightarrow OX + pH_2O, \quad (4)$$

where m', n', and p denote the stoichiometric coefficients of the reaction. If the surface reaction is rate-determining, the formation rate of OX at reduction time t_r is

expressed as

$$R = k'[PR_{ad}]^m[O_s]^n, \quad (5)$$

where k' is a rate constant, and m and n are reaction orders. The concentration of reactive oxygen actually available at the surface, $[O_s]$, was approximated by

$$[O_s] = A\{1 - (Y/Y_\infty)\}, \quad (6)$$

where Y and Y_∞ are the amounts of oxygen consumed up to $t_r = t_r$ and $t_r = \infty$, respectively. The proportionality constant A represents the initial surface concentration of reactive oxygen.

As for $[PR_{ad}]$, two cases are discerned depending on whether propylene adsorbs on exposed metal ions or on surface O_s. If it is assumed that the surface metal ions are all covered with oxygen at $t_r = 0$ and become uncovered by reduction, their concentration is given by

$$[M_s] = A - [O_s]. \quad (7)$$

In case propylene adsorbs on these exposed metal ions in a Langmuir-type manner, Eq. (5) can be expressed as follows:

$$R_1 = k'(A/Y_\infty)^{m+n} \times [KP_{PR}/(1 + KP_{PR})]^m Y^m (Y_\infty - Y)^n, \quad (8)$$

where P_{PR} and K are the partial pressure and equilibrium adsorption constant of propylene, respectively. When P_{PR} is kept constant, Eq. (8) is rewritten as

$$R_1 = k_1 Y^m (Y_\infty - Y)^n, \quad (9)$$

with k_1 being constant. Similarly, in case propylene adsorbs on O_s, the formation rate is given by

$$R_2 = k_2 (Y_\infty - Y)^{m+n}. \quad (10)$$

It was found that Eq. (9) was well fit to the rate of 1,5-hexadiene formation in the reduction of ZnO as shown in Fig. 1. The dotted line in the figure is an analytical curve drawn according to

$$R_{HD} = 1.8 \times 10^{-5} Y^{2.0} (Y_\infty - Y)^{2.1} \ \mu\text{mol/g}\cdot\text{min}, \quad (11)$$

where $Y = 28\ \mu$mol O/g. This equation indicates that the rate-determining reaction requires two exposed metal ions ($m = 2$) and two reactive oxygen atoms ($n = 2$). This picture is consistent with the previous proposal (*12*) that the coupling of two allylic intermediates leads to the 1,5-hexadiene formation. The reaction order m can also be determined from the effect of P_{PR} on R_{HD} by using Eq. (8). This gave $m = 2.1$ in good agreement with the above value $m = 2.0$.

The applicability of Eq. (10) is less clear. However, the fact that the CO_2 formation decreases monotonically with an increase in reduction degree for any group (I) oxides is compatible with Eq. (12). This suggests that the propylene molecules adsorbed on the reactive oxygen are converted to CO_2.

Reduction Behavior of Group (II) Oxides

The reduction behavior of group (II) oxides is discussed rather qualitatively because the phenomena are not so simple. First we are concerned with the change of reduction rate during reduction. As have been observed, there are two types in the changes of reduction rate; i.e., the rate of oxygen consumption decreases monotonically or goes through maxima with the progress of reduction.

The former type includes the reduction of Bi_2O_3, Fe_2O_3, MnO_2 (Fig. 4), V_2O_5, and Co_3O_4 (up to CoO) (Fig. 3). Such rate decreases in the gas–solid reaction are usually caused either (i) by a decrease in area of gas–solid interface ("contracting sphere model") or (ii) by a decrease in mass transport through the product layer ("diffusion model"). For spherical and uniform particles, the corresponding reduction rate (r) is expressed by (12) or (13), respectively:

$$r = k_i(1 - \alpha)^{\frac{2}{3}}, \quad (12)$$

or

$$r = k_{ii}(1 - \alpha)^{\frac{1}{3}}/[1 - (1 - \alpha)^{\frac{1}{3}}], \quad (13)$$

where α is the degree of reduction, and k_i and k_{ii} are rate constants (*13*). Applicability of these expressions to the present reduction curves was, however, not very satisfactory, probably because the particles were neither spherical nor uniform. Nevertheless, it is important that the reduction curves for Eqs. (12) and (13) are convex and concave upward, respectively. The convex reduction curve of Bi_2O_3 suggests that the rate is controlled by the chemical reaction at the gas–solid interface. The concave reduction curves of Co_3O_4 to CoO and of Fe_2O_3 to Fe_3O_4, on the other hand, suggest that the rates are controlled by mass transport. It has been reported that, in the reduction of Co_3O_4 with hydrogen, the produced CoO has a topotactic relation with Co_3O_4 (*14*). It is inferred that the surface Co ions of Co_3O_4 (spinel) migrate inward to form CoO (NaCl structure), allowing surface oxide ions to react with propylene: The rate decrease in this case should correlate with an increase in diffusion distance of Co ions. The reduction of Fe_2O_3 to Fe_3O_4, however, requires a rather drastic structural rearrangement, and the observed rate decrease is likely to result from the increasing difficulty of gas diffusion. MnO_2 and V_2O_5 also show reduction curves of the concave type, but the consecutive nature of the reduction makes the analyses more difficult.

The case in which the reduction rate goes through maxima during reduction was typically observed in the reduction of CoO (Fig. 3) and MoO_3. Such reduction behavior has been reported in the reduction of CoO with hydrogen (*15*), and it is possible that the rate acceleration at the earlier stage of reduction of CoO is associated with the generation of growth nuclei of metallic phase as usually considered. However, the reduction behavior of MoO_3 and CuO is far more complex and its analyses are difficult at present.

Finally, a comment is added to the reaction selectivity during the reduction of group (II) oxides. It has been observed that the selectivity of propylene oxidation does not change so much as the reduction rate, at least in the early stage of reduction. This suggests that, while the number of the active sites for propylene oxidation increases or decreases, the nature of them remains unchanged. In the later stage where the lower oxide phases appear, however, the selectivity can vary remarkably as observed on MnO_2 and CuO. Over such oxide catalysts, it may be possible to control the selectivity of the catalytic oxidation if the reduction state of catalysts is kept suitable.

REFERENCES

1. Schuit, G. C. A., *Mem. Soc. Roy. Sci. Liege*, 6e Série, Tome I, Fasc. **4**, 227 (1971).
2. Batist, P. A., Prette, H. J., and Schuit, G. C. A., *J. Catal.* **15**, 267 (1969).
3. Egashira, M., Sumie, H., Sakamoto, T., and Seiyama, T., *Kogyo Kagaku Zasshi* **73**, 860 (1970).
4. Shchkin, V. P., Ven'yaminov, S. A., and Boreskov, G. K., *Kinet. Katal.* **12**, 547 (1971).
5. Fattore, V., Fuhrman, Z. A., Manara, G., and Notari, B., *J. Catal.* **37**, 215, 223 (1975).
6. Misono, M., Nozawa, Y., and Yoneda, Y., *in* "Proceedings, 6th Int. Congr. Catalysis, 1976," p. 386. Chem. Soc., London, 1977.
7. Massoth, F. E., and Scarpiello, D. A., *J. Catal.* **21**, 225 (1971).
8. Moro-oka, Y., and Ozaki, A., *J. Catal.* **5**, 116 (1966).
9. Seiyama, T., Yamazoe, N., and Egashira, M., *in* "Proceedings, 5th Int. Congr. Catalysis, 1972," p. 997. North-Holland, Amsterdam/London, 1973.
10. Barin, I., and Knacke, I., "Thermochemical Properties of Inorganic Substances." Springer-Verlag, Berlin, 1973.
11. Stull, D. R., Westrum, Fr. E. H., and Sinke, G. C., "The Chemical Thermodynamics of Organic Compounds." Wiley, New York, 1969.
12. Seiyama, T., Uda, T., Mochida, I., and Egashira, M., *J. Catal.* **34**, 29 (1974).
13. Hulbert, S. F., *J. Brit. Ceram. Soc.* **6**, 11 (1969).
14. Takada, T., Iwase, K., and Hayashi, T., "Powder Metallurgy," p. 176. Interscience, New York, 1961.
15. Verhoeven, W., and Delmon, B., *Bull. Soc. Chim. Fr.* **1966**, 3065, 3070 (1966).